Pharm Res (2011) 28:7–21
DOI 10.1007/s11095-010-0097-7

RESEARCH PAPER

Two-Layered Dissolving Microneedles for Percutaneous Delivery of Peptide/Protein Drugs in Rats

Keizo Fukushima • Ayaka Ise • Hiromi Morita • Ryo Hasegawa • Yukako Ito • Nobuyuki Sugioka • Kanji Takada

Received: 19 October 2009 / Accepted: 17 February 2010 / Published online: 19 March 2010

ABSTRACT

Purpose Feasibility study of two-layered dissolving microneedles for percutaneous delivery of peptide/proteins using recombinant human growth hormone (rhGH) and desmopressin (DDAVP).

Methods Two-layered dissolving microneedles were administered percutaneously to the rat skin. Plasma rhGH and DDAVP concentrations were measured by EIA and LC/MS/MS. *In vivo* dissolution and diffusion rates of drugs in the skin were studied using tracer dyes, lissamine green B (LG) for rhGH and evans blue (EB) for DDAVP. Diffusion of drugs vertically into the skin was studied using FITC-dextran (MW = 20 kDa)-loaded dissolving microneedles. Stability experiments were performed at −80°C and 4°C.

Results The absorption half-lives, $t_{1/2a}$, of rhGH and DDAVP from dissolving microneedles were 23.7 ± 4.3–28.9 ± 5.2 and 14.4 ± 2.9–14.1 ± 1.1 min; the extents of bioavailability were 72.8 ± 4.2–89.9 ± 10.0% and 90.0 ± 15.4–93.1 ± 10.3%, respectively. LG and EB disappeared from the administered site within 2 h and 3 h after administration. Five green fluorescein spots were detected at 15 s and enlarged transversally at 30 s. FITC-dextran was delivered into the microcapillaries at 5 min and 10 min. The rhGH and DDAVP were stable in dissolving microneedles for one month at −80°C and 4°C.

Conclusions Results suggest that the two-layered dissolving microneedles are useful as an immediate-release transdermal DDS for peptide/protein drugs.

K. Fukushima (✉) • A. Ise • H. Morita • R. Hasegawa • Y. Ito • N. Sugioka • K. Takada
Department of Pharmacokinetics, Kyoto Pharmaceutical University, Yamashina-ku,
Kyoto 607-8412, Japan
e-mail: keizo@mb.kyoto-phu.ac.jp

K. Takada
e-mail: takada@mb.kyoto-phu.ac.jp

KEY WORDS bioavailability · desmopressin (DDAVP) · dissolving microneedles · recombinant human growth hormone (rhGH) · transdermal delivery

INTRODUCTION

Although the possibility of synthesized peptide and recombinant protein drugs becoming available to treat intractable ailments is increasing, the complex structures of these peptide/proteins require special formulation as a pharmaceutical preparation. The current list of approved therapeutic peptide/protein drugs is growing rapidly because automated drug discovery and biotechnology production methods are creating new biochemical drugs for an expanding number of intractable ailments (1). Demand for delivery of such macromolecular biopharmaceuticals as peptide/protein drugs is increasing (2). Because oral administration of peptide/protein drugs is the most preferred mode, oral delivery of peptide/protein drugs has been attempted using protease inhibitors (3,4), absorption enhancers (5–7), bioadhesive polymer-modified liposomes (8), chitosan capsules (9) and water-in-oil-in-water double emulsions (10–13), bioadhesive DDS (14), and cell-penetrating peptides (15,16). However, oral peptide/protein DDS has not been developed yet because of low oral bioavailability (BA). Consequently, no such oral preparation has been launched onto the pharmaceutical market. To date, most are administered intravenously or subcutaneously by injection.

On the other hand, a percutaneous administration route is an attractive alternative method for the delivery of these drugs because of its many advantages: (1) less or no degradation by hydrolytic enzymes compared to that in the GI tract, (2) no first-pass effects of the liver associated

with oral delivery, (3) less or no pain compared to subcutaneous injection, (4) better convenience of administration than intravenous injection, (5) better and more continuously controlled delivery rate than that of oral or subcutaneous sustained-release preparations, and (6) easy removal if side-effects appear. Despite its many advantages, transdermal drug delivery systems (TDDSs) are severely limited by poor permeability of drugs through the human skin: most drugs do not permeate through the skin at therapeutically relevant rates.

Human skin comprises three layers: the stratum corneum, epidermis, and dermis. The first is the 10–15-μm-thick outer layer; it is dead tissue. The stratum corneum has a strong primary barrier function against exogenous compounds, including drugs. The second barrier is the viable epidermis (100–150 μm), which contains tissues such as living cells. However, no blood vessels exist in the epidermis. To increase the skin permeability of drugs, numerous approaches using chemical enhancers, electric fields, ultrasound, and thermal methods have been attempted (17–21). However, the success of these TDDSs has remained limited because of the strong barrier function of the skin, *i.e.*, low membrane permeability of drugs through the skin. On the other hand, the development of microfabrication technology has made it possible to produce microneedles, which dramatically increase the skin permeability of drugs. Coated microneedle array patch systems have been shown to increase the transdermal permeability of desmopressin (22). In addition, Prausnitz *et al.* demonstrated that the skin permeability of insulin was increased dramatically by microneedle technology in rats (23). Thereafter, the efficiency of microneedle technology on the percutaneous administration of drugs, such as recombinant human growth hormone (rhGH) (24), docetaxel (25), naltrexon (26), and 5-aminolevulinic acid (27), has been suggested.

Those microneedle TDDSs are of three types: (1) extremely small needles through which drug solution can be injected into the skin, (2) metallic and/or silastic microneedles onto which a surface drug is coated, and (3) metallic and/or silastic microneedles by which microconduits are made on the skin, after which a drug solution is applied following removal of the microneedles. These materials, silicon and metals, are not used in pharmaceutical preparations.

In contrast to those microneedles, we designed two-layered dissolving microneedles with water-soluble thread-forming biopolymers, such as chondroitin sulfate, dextran, hyaluronic acid, and albumin, used as the base. The drug was formulated as a solid dispersion. After the insertion of pen-type dissolving microneedle with 1–2 mm length and 0.4-mm diameter into the skin, the base immediately dissolved. The drug was released and absorbed into the systemic circulation with high absorption efficiency. High physiological availabilities (PAs) of 91.3–97.7% were obtained for insulin in mice (28) and of 81.5–102.3% for low molecular weight heparin (LMWH) in rats (29). Furthermore, high BAs of 87.5% were obtained for rhGH in rats (30) and of 82.1–99.4% for erythropoietin (EPO) in mice (31). The relative BA of interferon (IFN) against subcutaneous injection of IFN solution was 79.9–117.8% in rats (32). Relative PA of insulin was 90–99% in dogs (33). However, those pen-type dissolving microneedles needed an applicator to be inserted into the rat skin. To accelerate the development of dissolving microneedles as a pharmaceutical preparation, we designed a two-layered dissolving microneedle patch of 1.0×1.0 cm, on which 100 dissolving microneedles with 10 lines and 10 columns were formed (34). Each dissolving microneedle had 500 μm length and 300 μm diameter at its base. The drug was formulated at the acral portion of the dissolving microneedle, which was inserted into the region of the epidermis and/or epidermal/dermal junctions by pressing with fingers.

The feasibility of two-layered dissolving microneedles as a TDDS for peptide/protein drugs was investigated in this study using rhGH as a model protein drug and desmopressin (DDAVP) as a model peptide drug.

MATERIALS AND METHODS

Materials

The rhGH and acetonitrile (HPLC grade) were obtained from Wako Pure Chemical Industries Ltd. (Osaka, Japan). The DDAVP was obtained from Bachem AG (Bubendorf, Switzerland). Sodium chondroitin sulfate, dextran (MW = 50–70 kDa), evans blue (EB), trifluoroacetic acid, formic acid and ammonium acetate were obtained from Nacalai Tesque Inc. (Kyoto, Japan). Fluorescein isothiocyanate-labeled dextran (FITC-dextran, MW = 20 kDa) was obtained from Sigma Chemical Co. (St. Louis, MO, USA). Lissamine green B (LG) was obtained from MP Biomedicals (Illkirch-Graffenstaden, France). All other materials used were of reagent grade and were used as received. Male Wistar Hannover rats used in the study were obtained from Japan SLC Inc. (Hamamatsu, Japan). A standard solid-meal commercial food (LabDiet®; Nippon Nousan Ltd., Yokohama, Japan) was used.

Preparation of Dissolving Microneedle Patch and Intravenous Solutions

To make the dense drug solution, drug glue, the following mixtures were used: (1) 2.5 mg of rhGH, 0.5 mg of LG, and

17.5 mg of sodium chondroitin sulfate; (2) 2.5 mg of rhGH, 0.5 mg of LG, and 17.5 mg of dextran; (3) 5.0 mg of rhGH, 0.5 mg of LG, and 17.5 mg of sodium chondroitin sulfate; (4) 1.0 mg of DDAVP, 25 mg of sodium chondroitin sulfate, and 0.2 mg of EB; and (5) 2.5 mg of FITC-dextran and 17.5 mg of sodium chondroitin sulfate. To each mixture, 40 μl of distilled water was added and kneaded at room temperature. After the drug glue was degassed under reduced pressure, it was dispensed into a mold containing 100 inverted cone-shaped wells with an area of 1.0 cm^2. Each well had a depth of 500 μm and a diameter of 300 μm at its top. The mold was covered with a 300 g steel plate; then the drug glue was filled into the wells. After the plate was removed, glue made of either 15 mg of chondroitin sulfate or 15 mg of dextran and 25 ml of distilled water was painted over the mold. It was then dried under the pressure of the stainless steel plate for 3 h. Thereafter, the plate was removed, and dissolving microneedle patch was obtained by detaching with a supporting material, base.

The rhGH solution for intravenous injection study was prepared by dissolving 0.5 mg of rhGH with 200 ml of phosphate-buffered saline (PBS). The DDAVP solution for intravenous injection study was also prepared by dissolving 3.0 mg of DDAVP with 200 ml of PBS.

Microscopic Observation of Dissolving Microneedles

A dissolving microneedle patch containing rhGH and LG and/or DDAVP and EB was observed using a digital videomicroscope (VH-5500; Keyence Co. Ltd., Osaka, Japan) under normal light.

Drug Content in Dissolving Microneedle Patch

The rhGH and DDAVP were extracted from dissolving microneedle patches with 1.0 ml of 0.1 mM phosphate buffer, pH7.4; a 100 μl aliquot was used for the enzyme immunoassay (EIA) and HPLC assays described below.

In Vivo Absorption Experiments in Rats

Male Wistar Hannover rats, 336±18 g, were anesthetized with intraperitoneal injection of sodium pentobarbital, 50 mg/kg. One group consisted of 3–4 rats. At 5 min before drug administration, 0.25 ml of blank blood samples was obtained from the left jugular vein with a heparinized syringe. The hair on the abdominal region was removed with a shaver (ES7111; Panasonic Inc., Osaka, Japan). The dissolving microneedles were inserted to the skin by pressing the base with two fingers for 3 min without any treatment. At 5, 10, 15, 30, and 45 min and 1, 1.5, 2, 3, and 4 h after administration, 0.25 ml blood samples were collected from the left jugular vein. For the DDAVP experiment, the sampling times were 0, 5, 10, 15, and 30 min and 1, 2, 3, and 4 h.

By centrifuging at 12,000 rpm for 10 min at 4°C using a centrifuge, Kubota 1700 (Kubota, Tokyo, Japan), 100 μl plasma samples were obtained. The resultant plasma samples were stored at −80°C until analysis.

For the intravenous injection experiment, rhGH solution and DDAVP solution were injected, respectively, into the right jugular vein of rats at doses of 2.5 μg/kg for rhGH and 15.0 μg/kg for DDAVP.

After a 0.25-ml blank blood sample was obtained from the left jugular vein, additional blood samples of 0.25 ml were obtained at 2, 5, 10, 30, and 45 min for rhGH and at 2, 5, 10, 15, 30 min and 1, 2, 3, and 4 h for DDAVP using a heparinized syringe.

After centrifugation, plasma samples were obtained. All these plasma samples were immediately frozen in a deep freezer at −80°C until analysis.

In Vivo Release and Diffusion Experiment in the Rat Skin

Male Wistar Hannover rats, 343±25 g, were used. Under anesthesia with an intraperitoneal injection of sodium pentobarbital, 50 mg/kg, the hair covering the abdominal skin was removed using an electric shaver. Dissolving microneedles were administered to the skin. Before and after administration at 5 and 30 min, and at 1, 2, 3 and 24 h, the diffusion rates of the tracers—LG for the rhGH dissolving microneedles and EB for the DDAVP dissolving microneedles—to the horizontal direction from the administered site of the skin were recorded using a digital camera (D-200; Nikon Corp., Tokyo, Japan).

To study the diffusion rate of model drug, FITC-dextran, to the vertical direction of the rat skin, skin samples were obtained at 15 and 30 s and at 1, 2, 5 and 10 min after administration of the FITC-dextran dissolving microneedles to the rat skin. The skin samples were embedded (Histo Prep®; Fisher Scientific International, NJ, USA), frozen at −80°C in a deep-freezer, and sectioned using a microtome. The skin sections, approximately 20 μm, were mounted on glass slides. The slides of FITC-dextran-loaded rat skin were visualized—under normal light with no staining or treatment—through a 10× objective using a videomicroscope (VH-5500; Keyence Co. Ltd., Osaka, Japan) equipped with a filter for fluorescein observation. The excitation wavelength was 495 nm. All animal protocols were approved by the institutional animal care and use committee, and experiments were conducted in accordance with the Guidelines for Animal Experimentation, Kyoto Pharmaceutical University.

Stability Study

The dissolving microneedle patches were kept under two different conditions for 1 month: −80°C and 4°C. Thereafter, drugs were extracted from the patches with 20 ml of phosphate buffer, pH 7.4. The drug contents were measured using EIA and LC/MS/MS methods.

Assay Methods of rhGH and DDAVP in Plasma

The rhGH contents in plasma and dissolution medium were measured using EIA with an immunoassay kit (BioSource International Inc., California, USA). Specifically, the solid-phase enzyme, amplified-sensitivity immunoassay was performed on a microtiter plate. The rhGH concentration of the plasma samples was determined against a standard curve of rhGH in rat plasma. Variation of the assay was evaluated using data obtained for rhGH quality control samples prepared in rat plasma and the standard curve. The validation parameters of precision (CV less than 15%) and accuracy (recovery of ±20%) were acceptable, and the lower limit of quantitation (LOQ) was 0.04 ng/ml. The basal endogenous rhGH levels were measured to be zero in all animals. A plate shaker (Titramax 101; Heidolph Instruments GmbH, Germany) and plate washer (Dia-washer II; Dia-Iatron Co. Ltd., USA) were used. Absorbance was measured at 450 nm using a microplate reader (MTP-300 microplate reader; Corona Electric Co. Ltd., Japan).

The DDAVP contents in the plasma sample were measured by modifying mass spectrometric methods (35,36) following a solid phase extraction (37,38). The DDAVP extraction in plasma was performed using an Oasis® HLB 1 cc (30 mg) extraction cartridge (Waters Corp., Massachusetts, USA). In a 1.5 ml microtube, 100 µl of the spiked rat plasma sample was mixed with 200 µl of 10% trifluoroacetic acid (TFA). After centrifugation at 9000×*g* for 10 min, the supernatant was loaded to a C_{18} Sep-column that was pre-equilibrated by washing with acetonitrile (1 ml, once) followed by 1% formic acid (1 ml, three times). The column was washed with 1% formic acid (1 ml, three times), and the eluent was discarded. Then DDAVP was eluted with acetonitrile and 1% formic acid at a ratio of 6:4 (v/v; 1 ml, three times), and eluent was collected in a test tube and evaporated to dryness at 60°C under the flow of nitrogen gas. The residue was reconstituted with 100 µl of mobile phase, of which 50 µl was injected into the LC/MS/MS system, as described below.

The LC/MS/MS system consisted of an API 3200 triple quadrupole mass spectrometer equipped with turbo ion spray sample inlet as an interface for electrospray ionization (ESI), an analyst workstation (Applied Biosystems, CA, U.S.A.), a micropump (LC-10AD; Shimadzu Corp., Kyoto, Japan) and an automatic sample injector (AS8020; Tosoh Corp., Tokyo, Japan). The mobile phase, 10 mM ammonium acetate: acetonitrile (30:70, v/v), was degassed and pumped through an ODS column (2.1 mm i.d.×100 mm, 3 µm size, Quicksorb; Chemco Scientific, Co. Ltd., Osaka, Japan) at a flow rate of 0.2 ml/min. The column temperature was maintained at 25°C. For DDAVP detection, the transitions of m/z 1069.3→120.3 were optimized for the following conditions. Ionization occurred *via* the turbo ion spray inlet in the positive ion mode. The flow rates of nebulizer gas, curtain gas, and collision gas were set, respectively, at 8.0, 8.0, and 2.0 l/min. The ion spray voltage and temperature were set, respectively, at 5 kV and 500°C. The declustering potential, the entrance potential, the collision energy and the collision cell exit potential were set, respectively, at 111.0, 10.0, 123.0, and 2.3 V.

Pharmacokinetic Analysis

Pharmacokinetic parameter values such as rate constants including the first-order absorption rate constant, k_a, were determined from the plasma drug concentration *vs.* time data using one-compartment and two-compartment open models with first-order absorption process according to the standard method (39) using software (WinNonlin; Pharsight Corp., CA, USA). The maximum drug concentration, C_{max}, and the time to reach maximum concentration, T_{max}, were determined from the authentic plasma drug concentration *vs.* time data. The area under the plasma drug concentration *vs.* time curve, AUC, after percutaneous administration or intravenous injection was calculated using the linear trapezoidal rule up to the last measured drug concentration, $C_{p(last)}$, and was extrapolated to infinity by addition of the correction term $C_{p(last)}/k$, where k was the terminal elimination rate constant. The bioavailability (BA) of the drug from dissolving microneedle patch was calculated using the following equation.

$$BA(\%) = \left(AUC_{patch}/AUC_{i.v.}\right) \times \left(Dose_{i.v.}/Dose_{patch}\right) \times 100$$

Statistics

All values are expressed as their mean±S.E. Statistical differences were assumed to be significant when $p<0.05$ (student's unpaired *t*-test).

RESULTS

Physicochemical Properties of Dissolving Microneedles

The prepared typical dissolving microneedles containing rhGH and DDAVP are presented in Fig. 1, where chondroitin sulfate was used as the base polymer. In

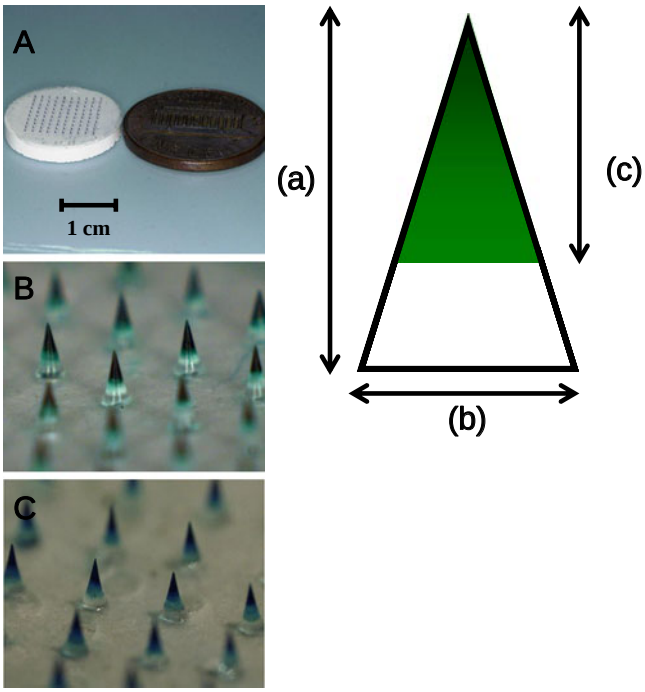

Fig. 1 Dissolving microneedles made of chondroitin sulfate as the base used in the *in vivo* rat absorption studies. **A** Overview image of dissolving microneedles. **B** rhGH chondroitin sulfate dissolving microneedles. **C** DDAVP chondroitin dissolving microneedles. The inserted schema shows the following length: (**a**) whole length, (**b**) diameter of the basement, and (**c**) length of the drug loaded space.

addition, the images of the enlarged dissolving microneedles are shown in the figure. With rhGH, dextran was also used to prepare the dissolving microneedles as the base. Because rhGH and DDAVP are transparent substances, tracer dyes, LG for the rhGH dissolving microneedles and EB for the DDAVP dissolving microneedles, were formulated with those drugs. At first, EB was used to prepare the rhGH dissolving microneedles. However, good transparency was not obtained. For that reason, LG was used instead of EB. As portrayed in those photos, both rhGH and DDAVP were formulated at the acral portion of dissolving microneedles. The physicochemical properties of the prepared dissolving microneedles are shown in Table I. The mean lengths of the dissolving microneedles were 477.5±12.9 μm and 483.5±2.5 μm for low and high content rhGH chondroitin sulfate dissolving microneedles, 497.3±0.6 μm for rhGH dextran dissolving microneedles and 488.8±3.4 μm for DDAVP chondroitin dissolving microneedles, respectively. The basement diameters were 295.0±4.2 μm and 285.6±2.3 μm for low and high rhGH content chondroitin dissolving microneedles, 285.8±2.9 μm for rhGH dextran dissolving microneedles and 290.6±6.8 μm for DDAVP chondroitin dissolving microneedles, respectively. The mean length of the drug-loaded space was 300.7±10.2 μm and 292.0±11.4 μm for low and high rhGH content chondroitin dissolving microneedles and 292.5±9.6 μm for rhGH dextran dissolving microneedles and 275.2±11.2 μm for DDAVP chondroitin dissolving microneedles from the top of the dissolving microneedles. The drug contents were 33.6±1.9 μg and 55.0±2.2 μg for low and high rhGH content chondroitin dissolving microneedles, 28.4±1.0 μg for rhGH dextran dissolving microneedles, and 5.2±0.4 μg for DDAVP chondroitin dissolving microneedles, respectively.

In Vivo Absorption of rhGH From Dissolving Microneedles in Rats

The obtained dissolving microneedles were administered to the rat skin by pressing the patch on the abdominal skin where the hair had been removed. Fig. 2 shows the plasma rhGH concentration *vs.* time curves after administration to rats with two preparations, chondroitin dissolving microneedles and dextran dissolving microneedles, with respective rhGH doses of 33.6±1.9 μg and 28.4±1.0 μg. The plasma rhGH concentration increased rapidly and reached its maximum concentrations at 15 min in both preparations. The maximum plasma rhGH concentrations, C_{max}, were 73.1±3.1 ng/ml for the low-content chondroitin dissolving microneedles and 58.4±5.6 ng/ml for the dextran dissolving microneedles, respectively (Table II). Thereafter, the plasma rhGH concentration gradually decreased and disappeared within 4 h after administration. No significant difference was found on the plasma rhGH concentration *vs.* time profiles between the two prepara-

Table I Physicochemical Property of Dissolving Microneedles Containing rhGH and DDAVP

Preparation code	Base	Drug	Drug content (μg)	Height (a)[a] (μm)	Base diameter (b)[a] (μm)	Drug-loaded space (c)[a] (μm)
GH dextran	Dextran	rhGH	28.4±1.0	497.3±0.6	285.8±2.9	292.5±9.6
GH chondroitin	Chondroitin	rhGH	33.6±1.9	477.5±12.9	295.0±4.2	300.7±10.2
GH chondroitin high	Chondroitin	rhGH	55.0±2.2	483.5±2.5	285.6±2.3	292.0±11.4
DDAVP chondroitin	Chondroitin	DDAVP	5.2±0.4	488.8±3.4	290.6±6.8	275.2±11.2

Each point shows the mean±S.E. of 3–6 experiments.

[a] The alphabets inside the parentheses represent the corresponding length in Fig. 1.

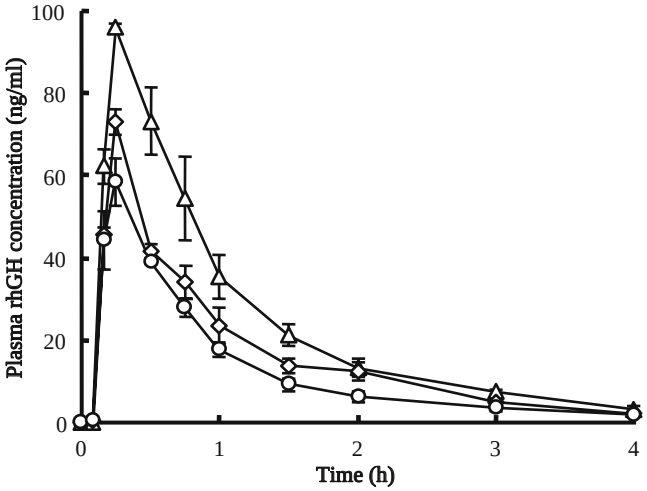

Fig. 2 Plasma rhGH concentration *vs.* time profiles after percutaneous administration of rhGH dissolving microneedles to the abdominal rat skin. Plasma rhGH concentrations were measured by EIA. The *open circle* denotes data obtained after administration of dextran dissolving microneedles containing 28.4±1.0 μg of rhGH. The open diamond denotes data for chondroitin dissolving microneedles containing 33.6±1.9 μg of rhGH. The *open triangle* denotes chondroitin dissolving microneedles containing 55.0±2.2 μg of rhGH. Each point represents the mean±S.E. of 3–4 experiments.

tions. To characterize the pharmacokinetics of rhGH after percutaneous administration to rats by dissolving microneedles, the plasma rhGH concentration *vs.* time data are shown on a semilogarithmic scale (Fig. 3). As the figure shows, plasma rhGH concentrations declined monoexponentially after the plasma rhGH concentration reached C_{max}. Therefore, the obtained elimination half-lives, $t_{1/2}$, were 28.9±5.2 min for low content chondroitin dissolving microneedles and 23.7±4.3 min for dextran dissolving microneedles, respectively. On the other hand, the rhGH solution was intravenously injected to another group of rats, 2.5 μg/kg. The plasma rhGH concentration *vs.* time curve is depicted in Fig. 3. Immediately after intravenous injection of rhGH solution, plasma rhGH concentration of 19.6±0.6 ng/ml was obtained at 2 min and plasma rhGH concentration declined with a first-order manner, where the elimination $t_{1/2}$ was 4.4±0.2 min. By comparing the elimination $t_{1/2}$ of rhGH obtained after percutaneous administration with dissolving microneedles, 23.7–28.9 min, with that obtained after intravenous injection of rhGH solution, a flip-flop phenomenon was thought to occur. Therefore, pharmacokinetic analysis using a one-compartment open model with first-order absorption rate process including flip-flop phenomenon was performed. The obtained pharmacokinetic parameter values are shown in Table II. The first-order absorption rate constant, k_a, of rhGH from dissolving microneedles was 1.52±0.24 h^{-1} for the low content chondroitin dissolving microneedles and 1.91±0.42 h^{-1} for the dextran dissolving microneedles, respectively. By calculating the half-lives at the absorption phase, $t_{1/2a}$, 28.9±5.2 min for low chondroitin dissolving microneedles and 23.7±4.3 min for dextran dissolving microneedles were obtained. Therefore, a high absorption rate of rhGH from dissolving microneedles was suggested. When a high content rhGH chondroitin dissolving microneedles, 55.0±2.2 μg, was administered to rats, plasma rhGH concentrations increased as presented in Fig. 2. The pharmacokinetic profile depicted in Fig. 3 also showed a flip-flop phenomenon. The pharmacokinetic parameter values were also determined as shown in Table II. No significant difference was found on k_a, k, and $t_{1/2}$ between the two chondroitin dissolving microneedles containing different amounts of rhGH. The AUC was increased in proportion to the rhGH dose, and the obtained AUC values of rhGH from dissolving microneedles were 66.1±7.4 and 95.9±8.1 ng·h/ml, respectively. In addition, C_{max} increased from 73.1±3.1 to 96.0±0.8 ng/ml, respectively. Therefore, both AUC and C_{max} were increased in

Table II Pharmacokinetic Parameters of rhGH After Percutaneous Administration of Dissolving Microneedles to Rats

Preparation code	k_a (1/h)	$t_{1/2a}$ (min)	k (1/h)	$t_{1/2}$ (min)	C_{max} (ng/ml)	T_{max} (min)	AUC (ng-h/ml)	BA (%)
GH dextran	1.91±0.42	23.67±4.31	9.25±1.35	4.68±6.12	58.4±5.6	15.0±0	50.6±2.9	72.8±4.2
GH chondroitin	1.52±0.24	28.93±5.15	10.51±0.54	3.96±0.24	73.1±3.1	15.0±0	66.1±7.4	89.9±10.0
GH chondroitin high	1.60±0.19	26.69±2.90	8.16±1.17	5.34±0.90	96.0±0.8^{**a}	15.0±0	95.9±8.1^{**a}	101.3±9.2

Each point shows the mean±S.E. of 3–4 experiments.

** $p<0.01$; significantly different against "GH dextran" preparation

^{a} $p<0.05$; significantly different against "GH chondroitin" preparation

k_a; first-order absorption rate constant

$t_{1/2a}$; absorption half-life

k; elimination rate constant

$t_{1/2}$; elimination half-life

AUC; area under the plasma drug concentration *vs.* time curve

BA; extent of bioavailability

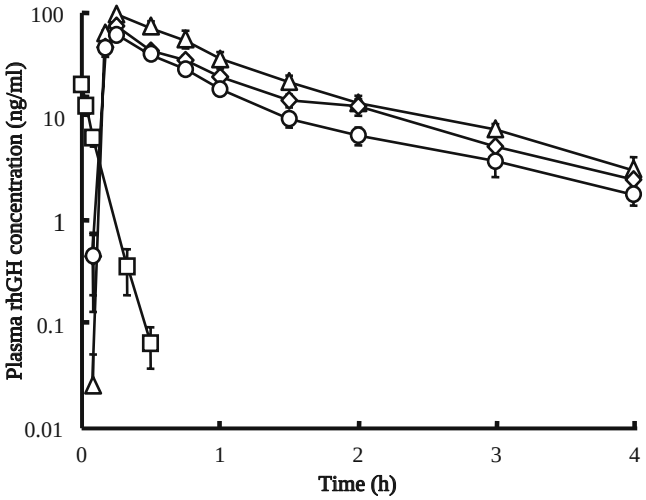

Fig. 3 Plasma rhGH concentration *vs.* time profiles in semilogarithmic scale after percutaneous administration of rhGH dissolving microneedles to the abdominal rat. The *open square* denotes data obtained after intravenous injection of rhGH solution to rats, 2.5 μg/kg. Other graphic characters are the same as those presented in Fig. 2.

proportion to the rhGH amount in chondroitin dissolving microneedles. To obtain the BAs of rhGH from chondroitin dissolving microneedles, those AUC values were compared to AUC obtained after intravenous injection of rhGH solution, 2.97±0.13 ng·h/ml. The estimated BA values were 89.9± 10.0% and 101.3±9.2% for low and high content chondroitin dissolving microneedles and 72.8±4.2% for dextran dissolving microneedles. The results suggested that chondroitin sulfate was better than dextran for use as the base of rhGH dissolving microneedles.

In Vivo Absorption of DDAVP From Dissolving Microneedles in Rats

Fig. 4 portrays the plasma DDAVP concentration *vs.* time curves after administration of 1 and 2 patches of chondroitin dissolving microneedles to rats, 5.2 μg and 10.4 μg. Plasma DDAVP concentrations also increased rapidly after administration and reached C_{max} at 30 min in both cases. The C_{max}s of DDAVP was 16.4±2.5 ng/ml for one-patch study and 27.3±2.4 ng/ml for two-patch study, respectively. Thereafter, plasma DDAVP concentration decreased gradually and disappeared within 4 h after administration. In addition, the DDAVP solution was intravenously injected to another group of rats, 15.0 μg/kg; the plasma DDAVP concentration *vs.* time curve is also presented in Fig. 4. For DDAVP, no flip-flop phenomenon was observed. Pharmacokinetic parameter values, shown in Table III, were calculated based on a two-compartment open model with first-order absorption processes. The C_{max}s of DDAVP was 16.4±2.5 ng/ml for the one-patch study and 27.3±2.4 ng/ml for the two-patch study, respectively. The first-order absorption rate constants, k_a, of DDAVP from the dissolving microneedles were 2.78±0.50 h^{-1} and 2.99±0.21 h^{-1}, respectively The absorption half-lives, $t_{1/2a}$, were 14.4±2.9 min and 14.1± 1.1 min, respectively. Therefore, DDAVP showed a higher absorption rate than rhGH from chondroitin dissolving microneedles. In addition, the BA values were 90.0±15.4% for the one-patch study and 93.1±10.3% for the two-patch study, respectively.

Release and Diffusion Study in Rat Skin

Figs. 5 and 6, respectively, show the results of *in vivo* dissolution and diffusion profile of the tracer dyes, LG for rhGH chondroitin dissolving microneedles and EB for DDAVP chondroitin dissolving microneedles, into the horizontal angle in the skin. After administration to rat skin, color spots were detected at 5 min, which suggested that the labeled acral portions of dissolving microneedles were inserted into the rat skin. As time passed, the color decreased because of the diffusion of tracer dyes into the skin. The LG and EB disappeared from the skin at 2 h and 3 h after administration, respectively. At 24 h after administration of chondroitin dissolving microneedles, the rat skin returned to the normal state. The kinetics of tracer dyes in the rat skin was well correlated to the kinetics of both drugs in the plasma, because both rhGH and DDAVP disappeared from the rat plasma within 4 h after percutaneous administration by chondroitin dissolving microneedles.

Fig. 7 portrays normal and fluorescent images of rat skin sections obtained after the administration of FITC-dextran

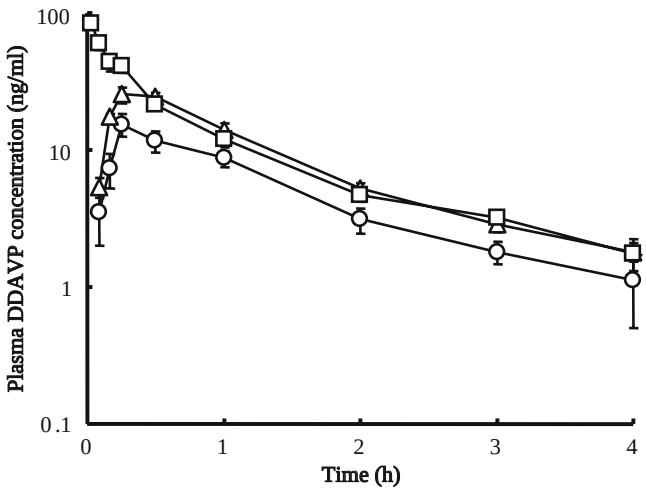

Fig. 4 Plasma DDAVP concentration *vs.* time profiles in semilogarithmic scale after percutaneous administration of DDAVP dissolving microneedles to the abdominal rat skin. The *open circle* denotes data obtained after administration of one patch of chondroitin dissolving microneedles, 5.2 μg of DDAVP. The *open triangle* denotes data for two patches of chondroitin dissolving microneedles, 10.4 μg of DDAVP. The *open square* denotes data obtained after intravenous injection of DDAVP solution to rats, 15 μg/kg. Each point represents the mean±S.E. of 3–4 experiments.

Table III Pharmacokinetic Parameters of DDAVP After Percutaneous Administration of Chondroitin Dissolving Microneedles to Rats

Number of preparation	k_a (1/h)	$t_{1/2a}$ (min)	k_{12} (min)	k_{21} (min)	k (1/h)	$t_{1/2}$ (min)	C_{max} (ng/ml)	T_{max} (min)	AUC (ng-h/ml)	BA (%)
1 patch	2.78 ± 0.50	14.38 ± 2.94	1.03 ± 0.33	1.22 ± 0.41	1.67 ± 0.24	117.91 ± 49.83	16.4 ± 2.5	27.5 ± 3.6	21.6 ± 2.8	90.0 ± 15.4
2 patches	2.99 ± 0.21	14.11 ± 1.10	1.07 ± 0.18	0.94 ± 0.23	1.48 ± 0.15	127.18 ± 32.78	27.3 ± 2.4**	25.2 ± 1.8	38.1 ± 2.2**	93.1 ± 10.3

Each point shows the mean ± S.E. of 3–4 experiments.

**$p < 0.01$; significantly different against 1 patch administration

k_{12}: transfer rate constant from central to peripheral compartment

k_{21}: transfer rate constant from peripheral to central compartment

dissolving microneedles to the rat skin. Because the MW of rhGH was 22 kDa, FITC-dextran with the MW of 20 kDa was used as a tracer. We performed the *in vivo* diffusion study by fluorescence imaging technology using dissolving microneedles containing FITC-insulin, MW = 6 kDa, and FITC-dextrans with MW of 4 kDa to 150 kDa. There was no significant difference on the fluorescence image between FITC-insulin and FITC-dextrans of which MW was 4 kDa to 20 kDa. We also performed the *in vitro* permeation experiment using stripped rat skin using FITC-dextrans with different MW, 10, 20, 40 and 70 kDa. The permeability coefficients were 4.59, 4.69, 3.38 and 1.43 ($\times 10^4$ cm/h), respectively. As the MW of FITC-dextran increased above 40 kDa, the permeability coefficients decreased. However, in the lower MW range, 10–20 kDa, there was not a difference on permeability coefficients (40). Although we tried to obtain FITC-rhGH, it was difficult to obtain it. Therefore, FITC-dextran, MW = 20 kDa, was used in this study. The green fluorescence derived from FITC-dextran was immediately apparent, and it spread with time, as presented in the figure. Because chondroitin sulfate, a water-soluble thread-forming polymer, was used as the base polymer to prepare dissolving microneedles, the dissolution and release of green fluorescein occurred immediately after administration. Even at 15 s after administration, the conical shape of dissolving microneedles was not completely detected, although five spots of green fluorescein were detected. At 30 s after administration, five green fluorescence spots enlarged transversally. However, at 1 min after administration, green fluorescence expanded vertically, which means that FITC-dextran diffused from the epidermal to the dermal area of the rat skin. At 2 min, diffusion to the transverse direction reached to the steady state. Thereafter, the diffusion to the vertical direction was completed and FITC-dextran was delivered into micro-capillaries at 5 and 10 min after administration.

Stability of rhGH and DDAVP in Dissolving Microneedles

Table IV shows the stability of rhGH and DDAVP in dissolving microneedles. Under two different conditions, the remaining percentage amounts of rhGH after 1 month were

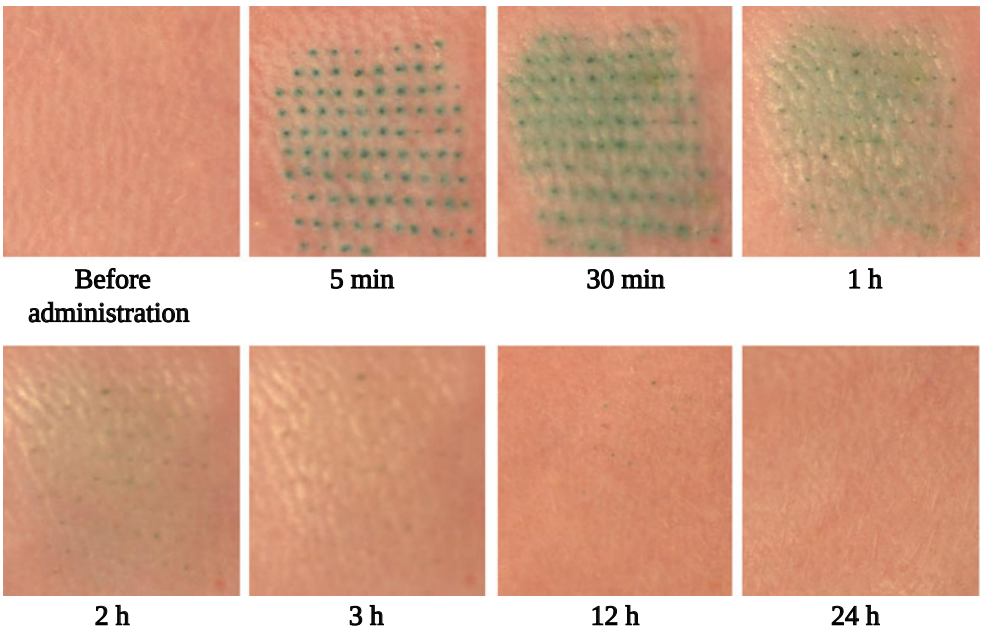

Fig. 5 *In vivo* dissolution and diffusion profile of the tracer dye, lissamine green (LG) for rhGH dissolving microneedles, into the horizontal angle in the skin. The dissolving microneedles were applied to rat abdominal skin and were removed at 1 min after administration.

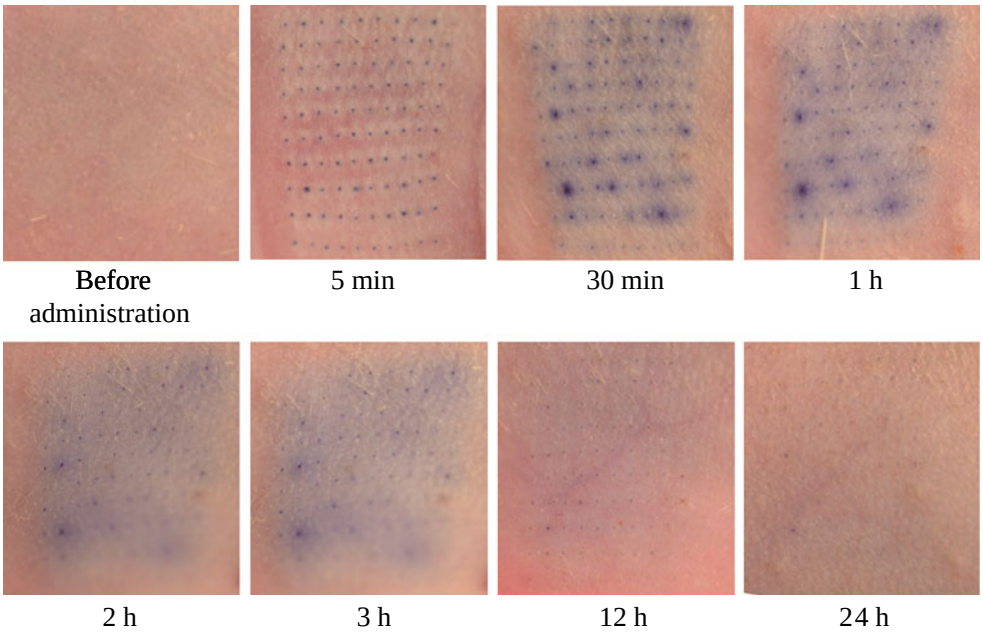

Fig. 6 *In vivo* dissolution and diffusion profile of the tracer dye, evans blue (EB) for DDAVP dissolving microneedles, into the horizontal angle in the skin. The dissolving microneedles were applied to rat abdominal skin and were removed at 1 min after administration.

98.2±3.9% (−80°C) and 99.7±1.5% (4°C), respectively. In the case of DDAVP dissolving microneedles, 101.1±1.7% (−80°C) and 100.0±1.9% (4°C) were recovered. Consequently, rhGH and DDAVP were found to be stable in dissolving microneedles for 1 month.

DISCUSSION

Design of Two-Layered Dissolving Microneedles

For this study, two kinds of rhGH dissolving microneedles, chondroitin and dextran microneedles, were prepared. Because the same mold was used to prepare both microneedles, no marked difference between the two dissolving microneedles was found in their shapes or sizes. The length of the drug-loading space was designed by considering the physiology of the skin. The epidermal thickness was reported to be 11.58±1.02 μm for rats and 22.47±2.40 μm for dogs (41). With respect to human skin, the epidermal thickness was reportedly 60.3±15.0 μm (42). Therefore, the lengths of the drug-loading space of dissolving microneedles were far longer than the epidermal thickness. The dermal region of the skin contains microcapillary and pain receptors found in deeper tissue. Clinical phase I study showed the safety of microneedles of 620 μm length and 160 μm width at the base (43). Our experiment showed that the whole dissolving microneedles, of which the length was approximately 500 μm, was not inserted into the skin. The acral portion of dissolving microneedles was inserted into the skin. Therefore, we designed 500 μm dissolving microneedles in which drug was localized at the acral portion of dissolving microneedles. It can deliver the drug to the epidermal and epiderm/dermal junction. When the dissolving microneedles were inserted to the rat skin, bleeding was not detected in this experiment, because dissolving microneedles were made of water-soluble thread-forming biopolymers (chondroitin sulfate or dextran), dyes (LG or EB) and drugs (rhGH or DDAVP). Those components were all water-soluble compounds. In addition, the dissolving microneedles was conical; the tops of dissolving microneedles were very narrow, approximately 10 μm. Therefore, after insertion of dissolving microneedles into the skin, hydration and dissolution occurred at the acral portion of dissolving microneedles as portrayed in Fig. 7. An approximately 300 μm length from the top of dissolving microneedles was inserted into the skin, where dissolving microneedles encountered environmental water: Caspers *et al.* reported that the water content in the skin was as high as 70% (44). In our previous report, pharmacokinetic evaluation of dissolving microneedles containing erythropoietin (EPO) was performed in rats and dogs, and species difference was studied (45). Higher BA of EPO was obtained in dogs, 65.9–69%, than in rats, 39.4%. By comparing the lengths of the recovered microneedles after administration, it was revealed that larger volume of the distal portion of the microneedles were dissolved and absorbed into the dog skin than in the rat skin. The absorbed volumes of the distal portion of the microneedles were $15.8\pm1.2\times10^5\mu m^3$ in the dog and $8.2\pm0.6\times10^5\mu m^3$ in rats. As the epidermal thickness of dogs is 2 times thicker than that of rats, dissolving microneedles were more fully inserted into the dog skin, and the higher BA of EPO was obtained in dogs than in rats. In the case of human, the epidermal thickness is

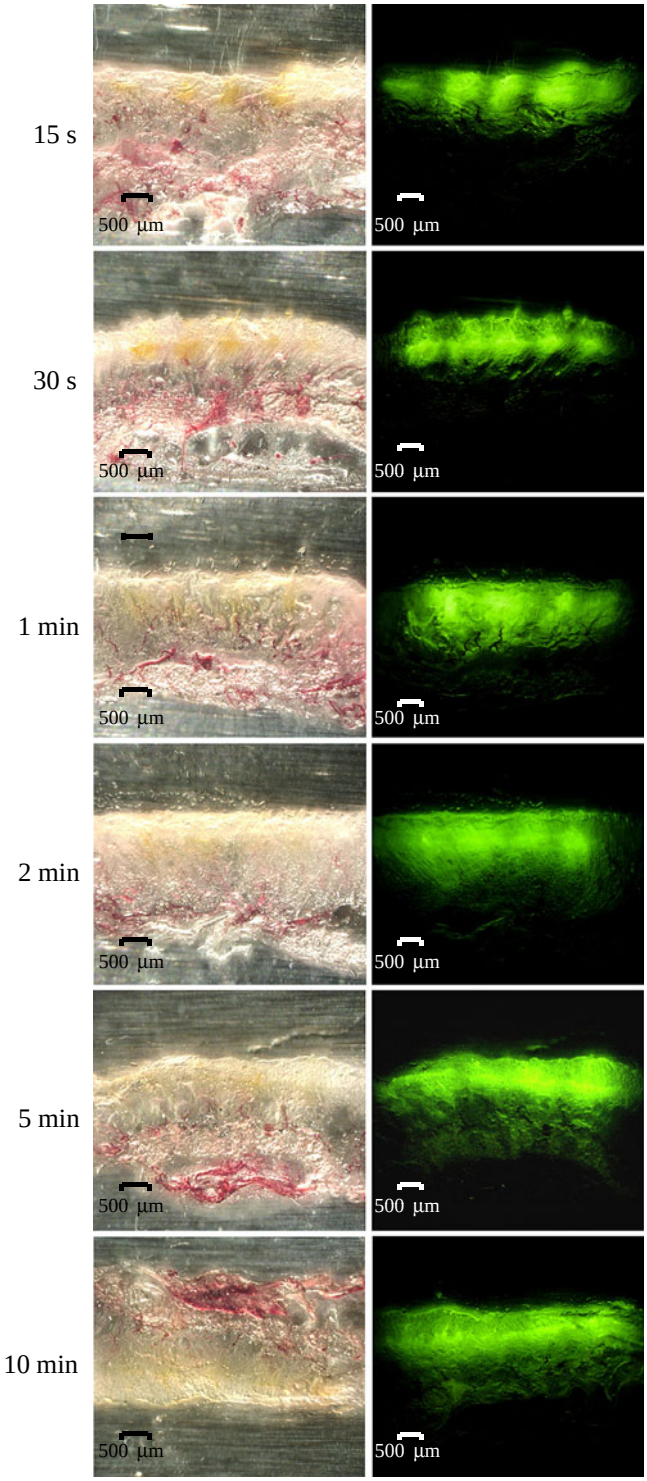

Fig. 7 Fluorescence videomicroscopy of the rat skin that received the chondroitin dissolving microneedles containing FITC-dextran (MW = 20 kDa) as visualized through a 10× objective (scale bar: 500 μm). The FITC-dextran chondroitin dissolving microneedles was administered to the rat abdominal skin. Thereafter, skin samples were obtained at 15 and 30 s and at 1, 2, 5 and 10 min. Left photographs show the corresponding brightfield microscopy images.

Table IV Stability of rhGH and DDAVP Chondroitin Dissolving Microneedles After 1 month

Drug	Temperature	
	−80°C (%)	4°C (%)
rhGH	98.2 ± 3.9	99.7 ± 1.5
DDAVP	101.1 ± 1.7	100.0 ± 1.9

Each point shows the mean ± S.E. of 5 experiments.

60.3 ± 15.0 μm. Therefore, higher BA is thought to be obtained.

Kolli *et al.* studied the transdermal delivery of nicardipine hydrochloride after microconduits were made by the insertion of microneedles onto the rat abdominal skin (46). In addition, Wermeling *et al.* described the appearance of a skin-impermeant drug, naltrexone, into the systemic circulation after microconduits were made by insertion of a stainless-steel microneedle sheet onto the human skin, where naltrexone was applied using a patch preparation (47). In their studies, plasma drug concentrations were measured, giving evidence that nicardipine and naltrexone were absorbed from the skin into the systemic circulation. However, precise evaluation related to the BA of drugs was not done. In contrast, our dissolving microneedles contained the drug in itself, and drug molecules existed in the dissolving microneedles as a solid dispersion. Solid dispersion technology is used to increase the solubility of hydrophobic compounds. Consequently, BAs of the drugs were increased considerably after oral administration (48–52). In the case of dissolving microneedles, solid dispersion technology was not intended to increase the solubility of the formulated drug, because both rhGH and DDAVP were water-soluble protein and peptide drugs. However, in accordance with solid dispersion technology, the dissolution rates of rhGH and DDAVP were very high, as shown by the high absorption rate constants, 1.52–1.60 h^{-1} and 2.78–2.99 h^{-1}, observed in the pharmacokinetic experiments. Therefore, we might state that one advantage of the dissolving microneedles is the rapid attainment of pharmacological activity after administration to the skin. In this study, dissolving microneedles containing rhGH and DDAVP were evaluated in rat experiment. The drug contents in the test dissolving microneedles were 28.4 ± 1.0–55.0 ± 2.2 μg for rhGH dissolving microneedles and 5.2 ± 0.4 μg for DDAVP dissolving microneedles, respectively. As the clinical dose of rhGH is approximately 1.0 mg, much rhGH must be formulated into the dissolving microneedles. One patch had 100 dissolving microneedles. The total weight of the acral portion of the dissolving microneedles was approximately 0.2 mg in which 0.1 mg of

rhGH could be formulated. Therefore, 1,000 dissolving microneedles are required for human patients. By increasing the surface area of patch, for example 10 cm^2, or increasing the rhGH content in dissolving microneedles, dissolving microneedle patch for clinical study can be prepared.

Rate and Extent of Bioavailability

To evaluate the pharmaceutical preparation, we must consider both the rate of bioavailability (RBA) and the extent of bioavailability (EBA). Levin *et al.* studied transdermal delivery of rhGH through microchannels created by radiofrequency ablation (24). They did not measure the absolute BA; they measured the relative BA against subcutaneous injection of rhGH solution. High relative EBAs—75% in rats and 33% in guinea pigs—were reported. In our experiment, the absolute EBA of rhGH was measured: 89.9±10.0% and 101.3±9.2% for chondroitin dissolving microneedles and 72.8±4.2% for dextran dissolving microneedles. On the other hand, the RBA of rhGH by radio-frequency ablation is low compared to our results. Levin *et al.* used four rhGH doses in the rat experiment: 75, 150, 300 and 450 μg. At 4 h after application to the rat skin, T_{max} was attained. In the case of their subcutaneous injection study, T_{max} was 2 h. In the guinea pig experiment, T_{max} was 2 h after percutaneous application of rhGH, where the rhGH doses were 50, 150, 300, and 400 μg; T_{max} for subcutaneous injection study was 2 h. On the other hand, T_{max} of rhGH obtained in our study was shown at 15 min after the administration of rhGH chondroitin and dextran dissolving microneedles, respectively. Therefore, high RBA of rhGH was obtained in the dissolving microneedles because of the immediate release of rhGH from dissolving microneedles following the rapid dissolution of the water-soluble thread-forming polymer such as chondroitin sulfate and dextran in the administered skin epiderm. Levin *et al.* used an rhGH patch prepared using printing technology, where rhGH was present in a dry form on a backing liner. The absorption mechanism of rhGH from their preparation was explained from a powder form of rhGH. The rhGH was dissolved by fluid exuded from the created microchannels. As a consequence, a very high local concentration of rhGH solution was formed *in situ*. The delivery of the dissolved rhGH molecules was mediated through microchannels into viable tissues of the skin by diffusion across a steep concentration gradient. In contrast, rhGH was present in the dissolving microneedles as a solid dispersion. By pressing the dissolving microneedles on the rat skin, the dissolving microneedles were inserted into the skin. The base polymer dissolved within a few minutes, releasing rhGH into the epidermis or epidermal/dermal junction. It was then absorbed into systemic circulation. Therefore, high RBA of rhGH was obtained: T_{max} appeared at 15 min after administration of the dissolving microneedles and a flip-flop phenomenon occurred. On the other hand, nasal and oral DDSs have been attempted with rhGH (53–57). Cheng *et al.* designed an intranasal chitosan/rhGH formulation, and EBA was evaluated in sheep, although the EBA was around 15% (53). The EBA of rhGH from the oral formulation was lower than that obtained from nasal absorption, although no EBA value was shown (54–57). Therefore, the dissolving microneedles will be a useful DDS for the systemic delivery of rhGH because higher EBA and RBA were obtained than other rhGH delivery systems.

With respect to DDAVP, nasal spray (58) is used clinically. In addition, sublingual spray has been attempted (59). However, very large intersubject variation on the plasma DDAVP concentration *vs.* time curves are reported. Cormier *et al.* (60) prepared a titanium microneedle array of which surface was coated with 82 μg of DDAVP. The absolute EBA was measured in hairless guinea pigs. High EBA, 85%, was obtained. However, RBA of DDAVP was not calculated because the blood sampling times were 0.5, 1, 2, 2.5, 4, and 6 h after administration to the skin. Because the serum DDAVP concentration at 1 h was slightly higher than the 0.5 h level, a slower absorption rate of DDAVP was observed for their coated microneedle array than for our DDAVP dissolving microneedles. As a coating solution, an aqueous formulation containing 24 or 40 w/v% DDAVP and 0.2 w/v% Polysorbate 20 was used. After drying, a solid layer was formed on the microneedle surface. On the other hand, DDAVP was formulated with a base polymer, chondroitin sulfate, and was microfabricated to the form of dissolving microneedles as a solid dispersion in our study. Therefore, higher RBA of DDAVP was obtained than when using a coated microneedle array system.

Penetration and Diffusion Rate in the Skin

The rate-limiting step of drug penetration into the skin is generally recognized to be the crossing step into the stratum corneum, the hydrophobic barrier of the skin (61). Because the barrier function of the stratum corneum is strong, not only hydrophilic low-molecular-weight organic compounds but also higher molecular weight peptide/proteins are difficult to be permeated into the dermis where microcapillaries exist. However, the dissolving microneedles physically remove the barrier of the stratum corneum and deliver drugs into the epidermis and epiderm/dermal junction. Therefore, the diffusion rate of drugs in the epidermal and dermal regions of the skin and permeation through the microcapillary wall is thought to be the rate-limiting step for absorption of drugs into systemic

circulation. To estimate the diffusion rate of drugs in the epidermal and dermal regions of the skin, a tracer experiment using FITC-dextran was performed. After insertion of the dissolving microneedles to the rat skin, green fluorescence derived from FITC-dextran increased immediately and diffused to the dermal region within 1 min. The diffusion of drugs through the dermal region occurred very rapidly, and plasma rhGH and DDAVP concentrations reached C_{max} at 15 min and 25.2–27.5 min, respectively. Especially in the case of rhGH, a flip-flop phenomenon was observed on its plasma concentration *vs.* time profiles.

Comparison with Other Microneedles

In our previous study, pen-type rhGH dissolving microneedle was used, and high BA, 87.5%, was obtained in the rat absorption experiment at rhGH dose of 250 μg/kg. To administer the pen-type dissolving microneedle, an applicator was used. In such a case, an applicator must be supplied to patients with dissolving microneedle, which increases medical fees. On the other hand, a dissolving microneedle patch was used in this study. The dissolving microneedles were applied to the rat skin by pressing with two fingers. The dissolving microneedles were easily inserted into the rat skin. Prior to our research, silicon microneedles were produced with microfabrication techniques. Chabri *et al.* prepared arrays of microconduits for direct and controlled access of molecules across the stratum corneum when inserted into the skin. The device enabled drugs to diffuse into the underlying viable epidermis and dermis (62). Furthermore, metallic microneedles were proposed. They are classifiable into two categories: hollow microneedles and microneedle arrays made of stainless steel (63) or titanium (64). Silastic and metallic microarrays are used in two ways. One method is the application of drug solution to the skin after physical conduits are made by the insertion of a metallic and/or silastic microarray. The second method is using a microarray of which the surface is coated with the drug. After the insertion of microarrays into the skin, the drug is dissolved and absorbed into the skin. On the other hand, hollow microneedles are developed, in which the drug solution is injected into the skin through hollow microneedles (65). As might be readily understood, these hollow microneedles are far from pharmaceuticals. Furthermore, in the case of metallic microneedles, the possibility exists of metallic allergy as suggested by Prausnitz *et al.* (66). Silicon microneedle arrays are fragile, the use of silicon is expensive, and silicon remains unproven as a biocompatible material. Therefore, these microneedles belong to the category of medical devices. On the other hand, dissolving microneedles satisfy the prerequisites of pharmaceuticals.

Safety of Dissolving Microneedles

With respect to the safety of dissolving microneedles, no damage or irritation on the rat skin was observed after the administration of the dissolving microneedles, as shown in Figs. 5 and 6. Our dissolving microneedles were made of water-soluble thread-forming polymer, chondroitin sulfate and dextran. Chondroitin sulfate is a peptideglycan that exists in biological tissues (67–72). Both chondroitin sulfate and dextran are used as an injection preparation. Dextran is used to treat peripheral circulatory disturbances in patients after head injury. Therefore, no safety problem exists when both biopolymers are used as the pharmaceutical additive for dissolving microneedles. Recently, Lee *et al.* prepared dissolving microneedles using carboxymethyl cellulose (CMC), amylopectin and bovine serum albumin (BSA) as the base (73). Recombinant BSA is now available. There is no problem related to its safety. However, because CMC is a pharmaceutical additive for oral preparation, safety studies must be performed to use it as the base for dissolving microneedles. Those polymers are also water-soluble thread-forming polymers. Consequently, study of the dissolving microneedles is increasing. To produce dissolving microneedles as a pharmaceutical preparation, safety must be established. In this study, histological observation of the administered skin was performed in addition to the *in vivo* dissolution and diffusion experiment. In both cases, the color attributable to the tracer dye was detected at the administered site of the rat skin up to 2–3 h after the administration of dissolving microneedles. However, irritation was not detected there. At 24 h after administration, the skin had recovered to a normal condition. Therefore, we must state that the dissolving microneedles are a reliable TDDS from the standpoint of safety. Peptide/protein drugs are very useful for patients. However, delivery systems are necessary for their more comfortable clinical use. The dissolving microneedles will be the solution to these clinical problems.

CONCLUSION

This feasibility study of dissolving microneedles with 500 μm length and 300 μm diameters of their basements was performed using rats. The dissolving microneedles were prepared with chondroitin sulfate and dextran as the base polymer using microfabrication technology. As protein/peptides, rhGH and DDAVP were formulated at the acral portion of dissolving microneedles. The rhGH contents in chondroitin dissolving microneedles and dextran dissolving microneedles were 33.6±1.9 μg and 28.4±1.0 μg, respectively. The chondroitin dissolving microneedles showed higher EBA (89.9±10.0%) than dextran dissolving microneedles (72.3±4.2%). As the absorption rate of rhGH was

fast, a flip-flop phenomenon was observed. The first-order absorption rate constant, k_a, was 1.52 ± 0.24 h^{-1} for chondroitin dissolving microneedles and 1.91 ± 0.42 h^{-1} for dextran dissolving microneedles. Plasma rhGH concentrations were well correlated to the formulated amount of rhGH in chondroitin dissolving microneedles. With DDAVP dissolving microneedles, high EBA (90.0–93.1%) and high RBA ($t_{1/2a}$ were 14.11–14.38 min) were obtained. The tracer dye, LG and EB, disappeared from the rat skin within 3 h after administration, and rhGH and DDAVP disappeared from the plasma within 4 h. A histological study of the administered skin showed no damage. In addition, the rhGH and DDAVP in dissolving microneedles were stable for 1 month at 4°C. The dissolving microneedles have been clarified as an advanced delivery system for the percutaneous delivery of rhGH and DDAVP.

ACKNOWLEDGMENTS

This study was supported by a strategic fund of MEXT (Ministry of Education, Culture, Sports, Science and Technology, MEXT) from 2008 to 2013 for establishing research foundation in private universities of Japan.

REFERENCES

1. Walsh G. Biopharmaceuticals. West Sussex: Wiley; 2003.
2. Shibata N, Ito Y, Takada K. Pharmacokinetics. In: Gad SC, editor. Handbook of pharmaceutical biotechnology. MA: Wiley-Interscience; 2007. p. 757–814.
3. Morishita I, Morishita M, Takayama K, Machida Y, Nagai T. Hypoglycemic effect of novel oral microspheres of insulin with protease inhibitor in normal and diabetic rats. Int J Pharm. 1992;78:9–16.
4. Yamamoto A, Taniguchi T, Rikyuu K, Tsuji T, Murakami M, Muranishi S. Effects of various protease inhibitors on the intestinal absorption and degradation of insulin in rats. Pharm Res. 1994;11:1496–500.
5. Amino Y, Kawada K, Toi K, Kumashiro I, Fukushima K. Phenylalanine derivatives enhancing intestinal absorption of insulin in mice. Chem Pharm Bull. 1988;36:4426–34.
6. Morishita M, Morishita I, Takayama K, Machida Y, Nagai T. Site dependent effect of aprotinin, sodium caprate Na_2EDTA and sodium glycocholate on intestinal absorption of insulin. Biol Pharm Bull. 1993;16:68–72.
7. Utoguchi N, Watanabe Y, Shida T, Matsumoto M. Nitric oxide donors enhance rectal absorption of macromolecules in rabbits. Pharm Res. 1998;15:870–6.
8. Takeuchi H, Yamamoto H, Niwa T, Hino T, Kawashima Y. Enteral absorption of insulin in rats from mucoadhesive chitosan coated liposomes. Pharm Res. 1996;13:896–901.
9. Tozaki H, Komoike J, Tada C, Maruyama T, Terabe A, Suzuki J. Chitosan capsules for colon-specific drug delivery: improvement of insulin absorption from the rat colon. J Pharm Sci. 1997;86:1016–21.
10. Matsuzawa A, Morishita M, Takayama K, Nagai T. Absorption of insulin using water-in-oil-in-water emulsion from an enteral loop in rats. Biol Pharm Bull. 1995;18:1718–23.
11. Cunha SA, Grossiord LJ, Puisieux F, Seiller M. Insulin in W/O/W multiple emulsions: biological activity after oral administration in normal and diabetic rats. J Microencapsul. 1997;14:321–33.
12. Morishita M, Matsuzawa A, Takayama K, Isowa K, Nagai T. Improving insulin enteral absorption using water-in-oil-in-water emulsion. Int J Pharm. 1998;172:189–98.
13. Suzuki A, Morishita M, Kajita M, Takayama K, Isowa K, Chiba Y, *et al.* Enhanced colonic and rectal absorption of insulin using a multiple emulsion containing eicosapentaenoic acid and docosahexaenoic acid. J Pharm Sci. 1998;87:1196–202.
14. Takada K. Oral delivery of haematopoietic factors: Progress with gastrointestinal mucoadhesive patches, microdevices and other microfabrication technologies. Am J Drug Deliv. 2006;4:65–77.
15. Khafagy El-S, Morishita M, Isowa K, Imai J, Takayama K. Effect of cell-penetrating peptides on the nasal absorption of insulin. J Control Release 2009;133:103–8.
16. Kamei N, Morishita M, Takayama K. Importance of intermolecular interaction on the improvement of intestinal therapeutic peptide/protein absorption using cell-penetrating peptides. J Control Release 2009;136:179–86.
17. Barry B, Williams A. Penetration enhancers. Adv Drug Deliv Rev. 2004;56:603–18.
18. Cevc G. Lipid vesicles and other colloids as drug carriers on the skin. Adv Drug Deliv Rev. 2004;56:675–711.
19. Preat V, Vanbever R. Skin electroporation for transdermal and topical delivery. Adv Drug Deliv Rev. 2004;56:659–74.
20. Doukas A. Transdermal delivery with a pressure wave. Adv Drug Deliv Rev. 2004;56:559–79.
21. Mitragotri S, Kost J. Low-frequency sonophoresis: a review. Adv Drug Deliv Rev. 2004;56:589–601.
22. Cormier M, Johnson B, Ameri M, Nyam K, Libiran L, Zhang DD, *et al.* Transdermal delivery of desmopressin using a coated microneedle array patch system. J Control Release 2004;97:503–11.
23. Prausnitz RM. Microneedles for transdermal drug delivery. Adv Drug Deliv Rev. 2004;56:581–7.
24. Levin G, Gershonowitz A, Sacks H, Stern M, Sherman A, Rudaev S, *et al.* Transdermal delivery of human growth hormone through RF-microchannels. Pharm Res. 2005;22:550–5.
25. Qiu Y, Gao Y, Hu K, Li F. Enhancement of skin permeation of docetaxel: A novel approach combining microneedle and elastic liposomes. J Control Release 2008;129:144–50.
26. Wermeling DP, Banks SL, Hudson DA, Gill HS, Gupta J, Prausnitz MR, *et al.* Microneedles permit transdermal delivery of a skin-impermeant medication to humans. Proc Natl Acad Sci USA. 2008;105:2058–63.
27. Donnelly RF, Morrow DIJ, McCarron PA, Woolfson AD, Morrissey A, Juzenas P, *et al.* Microneedle mediated intradermal delivery of 5-aminolevulinic acid: Potential for enhanced topical photodynamic therapy. J Control Release 2008;129:154–62.
28. Ito Y, Hagiwara E, Saeki A, Sugioka N, Takada K. Feasibility of microneedles for percutaneous absorption of insulin. Eur J Pharm Sci. 2006;29:82–8.
29. Ito Y, Murakami A, Maeda T, Sugioka N, Takada K. Evaluation of self-dissolving needles containing low molecular weight heparin (LMWH) in rats. Int J Pharm. 2008;349:124–9.
30. Ito Y, Ohashi Y, Shiroyama K, Sugioka N, Takada K. Self-dissolving micropiles for the percutaneous absorption of human growth hormone in rats. Biol Pharm Bull. 2008;31:1631–3.
31. Ito Y, Yoshimitsu J, Shiroyama K, Sugioka N, Takada K. Self-dissolving microneedles fir the percutaneous absorption of EPO in mice. J Drug Target 2006;14:255–62.
32. Ito Y, Saeki A, Shiroyama K, Sugioka N, Takada K. Percutaneous absorption of interferon-α by self-dissolving micropiles. J Drug Target 2008;16:243–9.

33. Ito Y, Ohashi Y, Saeki A, Sugioka N, Takada K. Antihyperglycemic effect of insulin from self-dissolving micropiles in dogs. Chem Pharm Bull. 2008;56:243–6.
34. Takada K. Microfabrication derived DDS: From batch to individual production. Drug Discov Ther. 2008;2:140–55.
35. Schmitz T, Huck CW, Bernkop-Schnurch A. Characterization of the thiol-disulphide chemistry of desmopressin by LC, μg-LC, LC-ESI-MS and Maldi-Tof. Amino Acids 2006;30:35–42.
36. Getie M, Neubert RH. LC-MS determination of desmopressin acetate in human skin samples. J Pharm Biomed Anal. 2004;35:921–7.
37. Kluge M, Riedl S, Erhart-Hofmann B, Hartmann J, Waldhauser F. Improved extraction procedure and RIA for determination of arginine8-vasopressin in plasma: role of premeasurement sample treatment and reference values in children. Clin Chem. 1999;45:98–103.
38. Agerso H, Seiding Larsen L, Riis A, Lovgren U, Karlsson MO, Senderovitz T. Pharmacokinetics and renal excretion of desmopressin after intravenous administration to healthy subjects and renally impaired patients. Br J Clin Pharmacol. 2004;58:352–8.
39. Gibaldi M, Perrier D. Pharmacokinetics. New York: Marcel Dekker; 2006.
40. Ito Y, Ise A, Sugioka N, Takada K. Molecular weight dependence on bioavailabity of FITC-dextran after administration of self-dissolving micropile to rat skin. Drug Dev Ind Pharm. in press (2010).
41. Monteiro-Riviere AN, Bristol GD, Manning OT, Rogers AR, Riviere EJ. Interspecies and interregional analysis of the comparative histologic thickness and laser Doppler blood flow measurements at five cutaneous sites in nine species. J Invest Dermatol. 1990;95:582–6.
42. Bauer J, Bahmer AF, Worl J, Neuhuber W, Schuler G, Fartasch M. A strikingly constant ration exists between Langerhans cells and other epidermal cells in human skin. A stereologic study using the optical dissector method and the confocal laser scanning microscope. J Invest Dermatol. 2001;116:313–8.
43. Wermeling PD, Banks LS, Hudson AD, Gill SH, Gupta J, Prausnitz RM, *et al.* Microneedles permit transdermal delivery of a skin-impermeant medication to human. Proc Natl Acad Sci USA. 2008;105:2058–2063.
44. Caspers JP, Lucassen WG, Bruining AH, Puppels JG. Automated depth-scanning confocal Raman microspectrometer for rapid *in vivo* determination of water concentration profiles in human skin. J Raman Spectrosc. 2000;31:813–8.
45. Ito Y, Hasegawa R, Fukushima K, Sugioka N, Takada K. Self-dissolving micropile array chip as percutaneous delivery system of protein drug. *Biol Pharm Bull*. in press (2010).
46. Kolli CS, Banga AK. Charcterization of solid maltose microneedles and their use for transdermal delivery. Pharm Res. 2007;25:104–13.
47. Wermeling PD, Banks LS, Hudson AD, Gill SH, Gupta J, Prausnitz RM, *et al.* Micropiles permit transdermal delivery of a skin-impermeant medication to humans. Proc Natl Acad Sci USA. 2008;105:2058–63.
48. Duan H-G, Wei Y-H, Li B-X, Qin H-Y, Wu X-A. Improving the dissolution and oral bioavailability of the poorly water-soluble drug aloe-emodin by solid dispersion with polyethylene glycol 6000. Drug Dev Res. 2009;70:363–9.
49. Park YJ, Kwon R, Quan ZQ, Oh HD, Kim OJ, Hwang RM, *et al.* Development of novel ibuprofen-loaded solid dispersion with improved bioavailability using aqueous solution. Arch Pharm Res. 2009;32:767–72.
50. Kennedy M, Hu J, Gao P, Li L, Ali-Reynolds A, Chal B, *et al.* Enhanced bioavailability of a poorly soluble VR1 antagonist using an amorphous solid dispersion approach: a case study. Mol Pharm. 2008;5:981–93.
51. Fukushima K, Haraya K, Terasaka S, Ito Y, Sugioka N, Takada K. Long-term pharmacokinetic efficacy and safety of low-dose ritonavir as a booster and atazanavir pharmaceutical formulation based on solid dispersion system in rats. Biol Pharm Bull. 2008;31:1209–14.
52. Vasconcelos T, Sarmento B, Costa P. Solid dispersions as strategy to improve oral bioavailability of poor water soluble drugs. Drug Discov Today 2007;12:1068–75.
53. Cheng YH, Dyer AM, Jabbal-Gill I, Hinchcliffe M, Nankervis R, Smith A, *et al.* Intranasal delivery of recombinant human growth hormone (somatropin) in sheep using chitosan-based powder formulations. Eur J Pharm Sci. 2005;26:9–15.
54. Moore JA, Pletcher SA, Ross MJ. Absorption enhancement of growth hormone from the gastrointestinal tract of rats. Int J Pharm. 1986;34:35–43.
55. Li H, Song JW, Park JS, Han K. Polyethylene glycol-coated liposomes for oral delivery of recombinant human epidermal growth factor. Int J Pharm. 2003;258:11–9.
56. Lam XM, Duenas ET, Cleland JL. Encapsulation and stabilization of nerve growth factor into poly (lactic-co-glycolic) acid microspheres. J Pharm Sci. 2001;90:1356–65.
57. Kim HK, Park TG. Microencapsulation of dissociable human growth hormone aggregates within poly (D, L-lactic-co-glycolic) acid microparticles for sustained release. Int J Pharm. 2001;229:107–16.
58. Joukhadar C, Schenk B, Kaehler ST, Kollenz CJ, Bauer P, Muller M, *et al.* A replicate study design for testing bioequivalence: a case study on two desmopressin nasal spray preparations. Eur J Clin Pharmacol. 2003;59:631–6.
59. Steiner IM, Kaehler ST, Sauermann R, Rinosl H, Muller M, Joukhadar C. Plasma pharmacokinetics of desmopressin following sublingual administration: an exploratory dose-escalation study in healthy male volunteers. Int J Clin Pharm Ther. 2006;44:172–9.
60. Cormier M, Johnson B, Ameri M, Nyam K, Libiran L, Zhang D, *et al.* Transdermal delivery of desmopressin using a coated microneedle array patch system. J Control Release 2004;97:503–11.
61. de Jager MW, Ponec M, Bouwstra JA. The lipid organization in stratum corneum and model systems based on ceramides. In: Touitou E, Barry BW, editors. Enhancement in drug delivery. London: CRC; 2007. p. 217–32.
62. Chabri F, Bouris K, Jones T, Barrow D, Hann A, Allender C, *et al.* Microfabricated silicon microneedles for nonviral cutancous gene delivery. Br J Dermatol. 2004;150:869–77.
63. Gardeniers HJGE, Luttge R, Berenschot EJW, de Boer MJ, Yeshurun SY, Hefetz M, van't Oever R, van den Berg A. Silicon micromachined hollow microneedles for transdermal liquid transport. J Microelectromech Syst. 2003;12:855–62.
64. Ito Y, Hagiwara E, Saeki A, Sugioka N, Takada K. Feasibility of microneedles for percutaneous absorption of insulin. Eur J Pharm Sci. 2006;29:82–8.
65. Davis PS, Martanto W, Allen GM, Prausnitz RM. Hollow metal micropiles for insulin delivery to diabetic rats. IEEE Trams Biomed Eng. 2005;52:909–15.
66. Arora A, Prausnitz MR, Mitragotri S. Micro-scale devices for transdermal drug delivery. Int J Pharm. 2008;364:227–36.
67. Morawski M, Alpár A, Brückner G, Fiedler A, Jäger C, Gati G, *et al.* Chondroitin sulfate proteoglycan-based extracellular matrix in chicken (Gallus domesticus) brain. Brain Res. 2009;1275: 10–23.
68. Faissner A, Clement A, Lochter A, Streit A, Mandl C, Schachner M. Isolation of a neural chondmitin sulfate proteoglycan with neurite outgrowth promoting properties. J Cell Biol. 1994;126:783–99.
69. Umehara Y, Yamada S, Nishimura S, Shioi J, Robakis NK, Sugahara K. Chondroitin sulfate of appican, the proteoglycan form of amyloid precursor protein, produced by C6 glioma cells interacts with heparin-binding neuroregulatory factors. FEBS Lett. 2004;557:233–8.

70. Wilson TM, Snow DM. Chondroitin sulfate proteoglycan expression pattern in hippocampal development: potential regulation of axon tract formation. J Comp Neurol. 2000;424:532–46.
71. Sintov A, Di-Capua N, Rubinstein A. Cross-linked chondroitin sulfate: characterization for drug delivery purposes. Biomaterials 1995;16:473–8.
72. Tsai FM, Chiang LY, Wang FL, Huang WG, Wu CP. Oral sustained delivery of diclofenac sodium using calcium chondroitin sulfate matrix. J Biomater Sci Polym Ed. 2005;16:1319–l331.
73. Lee JW, Park J-H, Prausnitz MR. Dissolving microneedles for transdermal drug delivery. Biomaterials 2008;29:2113–24.